scientific reports

Check for updates

OPEN

Understanding local connectivity and complexity in the skeleton of deforestation

Andrea Urgilez-Clavijo[1,2], David Andrés Rivas-Tabares[3,4], Anne Gobin[5], Ana María Tarquis Alfonso[3,6] & Juan de la Riva Fernández[1,7]✉

Current spatial analyses of deforestation predominantly focus on quantification, often overlooking the geometric and topological configurations that are essential for formulating spatially concrete remedial actions. Skeletons and local connected fractal dimension (LCFD) are established techniques that have been used to summarise geometric features and capture connectivity patterns. The present study analysed deforested areas in the Sumaco Biosphere Reserve at three time points from 1990 to 2018. The skeleton captured 62%, 44%, and 40% of the original deforested patches, respectively, and the complexity of connectivity patterns increased over time. A spatially explicit characterisation of the deforested patches was conducted by combining the LCFD and topological descriptors, which enabled the definition of five prioritisation levels for informed decision-making. In addition, we observed an increase in the complexity of pixel neighbourhood relationships over time. In conclusion, the spatial characterisation of the deforestation skeleton serves to further understand the dynamics of deforestation expansion from the local to the regional scale by highlighting complex connections that are significant for forest protection and mitigation efforts.

Deforestation is a global concern that impacts ecosystems, hydrologic and nutrient cycles, biodiversity, and climate. Extensive agriculture and urban growth are the main driving factors of this landscape change[1–4] since they promote forest loss. Halting deforestation is a management and policymaking challenge[5,6]. International agreements call for multidisciplinary initiatives to address this threat. Within the framework of Agenda 2030 and the Sustainable Development Goals (SDGs), especially SDG15 targets 15.2 and 15.b outline step for progress[7,8]. However, uncoordinated land management practices in tropical forests are exacerbating the process of deforestation.

Currently, the Amazon biome is worldwide recognised as a deforestation hotspot requiring immediate remedial action[9–11]. Patterns and complexity are common features of this process in time and space[12,13]. In the spatial sciences, the complexity of land processes deals with interactions between people and the environment resulting in land use and land cover (LULC) change[14]. Therefore, the study of LULC that has led to deforestation is crucial to understanding stakeholder land-use decisions[15] across spatially linked scales.

Deforestation exhibits complex spatial patterns with scale hierarchies and unexpected shapes. The land mosaic resulting from deforestation is characterised by intricate and irregular geometries, resembling fishbones at local scales[16,17], progressively expanding into regional patterns[18]. This cumulative process of deforestation[19–21] acts as a spatiotemporal disturbance event that modifies the geographic structure and composition of the ecosystem[22,23]. The sequence of spatial processes involved in land transformation, such as perforation, dissection, fragmentation, shrinkage, and attrition[24,25], collectively configure deforestation in a spatially complex manner. Over time, the combined effect of these processes, along with the influence of neighbouring deforested patches[26], promotes an exacerbated expansion of deforestation characterised by geometrically complex patterns.

The deforestation morphology configures several spatial patterns[27,28] of a complex system, leading to the irreversible progress of landscape fragmentation. The conventional study of forest fragmentation and connectivity includes the analysis of forest patch morphology using basic landscape ecology metrics[29–31] to

[1]Department of Geography and Land Management, GEOFOREST-IUCA, University of Zaragoza, 50009 Zaragoza, Spain. [2]Institute for Sectional Regime Studies of Ecuador (IERSE), Universidad del Azuay, 010204 Cuenca, Ecuador. [3]Research Centre for the Management of Agricultural and Environmental Risks (CEIGRAM), ETSIAAB, Universidad Politécnica de Madrid, 28040 Madrid, Spain. [4]GeoinfoRmatics, Agrosciences and Sustainable Solutions Group (GRASS), Faculty of Agricultural Sciences, School of Agronomy, Universidad de Cuenca, 010205 Cuenca, Ecuador. [5]Department of Earth and Environmental Sciences, KU Leuven, 3001 Leuven, Belgium. [6]Complex Systems Group (GSC), Universidad Politécnica de Madrid, 28040 Madrid, Spain. [7]Departamento de Geografía y Ordenación del Territorio, Universidad de Zaragoza, Pedro Cerbuna 12, 50009 Zaragoza, Spain. ✉email: delariva@unizar.es

fractal[26,32], particle[33], and succolarity analysis[34], among others. However, few studies focus on analysing vacant land once it has been deforested, termed deforested patches. These areas are subsequently occupied by other land uses, triggering adjacent land occupation effects. Similar to forest patches, deforested patches can be spatially characterised to understand their behavior in terms of fragmentation and connectivity.

Large-scale deforested areas can not be simply reforested due to contemporary socio-economic developments[35,36]. These areas are now complex land mosaics with different activities occurring concurrently. This situation necessitates an integrated restoration approach driven by local remedial actions[37]. Therefore, by using a spatial unit smaller than the entire deforested patch that aligns with LULC dynamics, an optimised trajectory can be developed to progressively restore landscape connectivity.

Remote sensing and image processing play a crucial role in supporting efforts to address environmental problems such as deforestation[38–42]. These technologies are being used to develop solutions that can assist decision-making and facilitate remedial actions[43]. In the context of deforestation, these tools have allowed studies from different disciplines[44]. However, significant gaps remain in our understanding of the underlying mechanisms driving the territorial expansion of deforestation. Diverse shape-analytical methods have focused on quantifying forest loss by analysing residual forest areas, neglecting the lost areas themselves. Mathematical morphology[45,46] provides an alternative approach to analysing these lost areas. This technique gained importance in geomorphology and GIS sciences as a powerful tool for generating reliable solutions to geomorphological phenomena and processes.

Image analysis has been established as a versatile technique for analysing both morphology and spatial patterns[47–49]. Morphological analysis provides image-derived shape features that can support decision-making across a wide range of disciplines including medicine[50], materials science[51], biology[52], geography[53], hydrology[54], soil science[55,56], among others. Spatial patterns, also known as spatial structures, refer to quantifiable attributes of how shapes are arranged in a spatial context[57], making them valuable for mapping and monitoring changes over time.

In binary image analysis, skeletonisation is a process that reduces shapes to a simplified, central structure while preserving their overall connectivity and topology. The skeleton is a thinned representation (i.e., one pixel wide) of an object's external morphology, capturing its fundamental structural framework while remaining relatively stable despite natural contour variations[58,59]. Deforested patches have internal geometric structures, or skeletons, which contain information about the original deforested patches. These structures can be used in spatial and temporal analyses across various land science disciplines, providing valuable insights into deforestation dynamics and informing land management strategies.

From an ecological perspective, the skeleton of deforested areas provides critical insights into the fragmentation and connectivity of landscapes. Deforestation alters habitat networks by breaking down continuous forest cover into isolated patches, affecting species movement, resource availability, and ecosystem stability[60]. Skeletonisation allows for the identification of primary connectivity pathways within deforested regions, highlighting corridors that may still facilitate species dispersal or gene flow. Additionally, the skeletal representation can help assess whether deforestation follows a structured pattern, such as linear clearing along roads or rivers, or a more diffuse, patchy expansion. Understanding these patterns is essential for designing effective conservation strategies, as maintaining or restoring connectivity between fragmented habitats is crucial for biodiversity conservation and ecological resilience[61]. A detailed explanation of skeletonisation and its implementation in this study is provided in the Methods section.

In addition, shape analysis enables the extraction of topological properties used for global descriptions of objects in an image. One such topological property is the number of connected components. This, calculated from the skeleton, provides information about the pixel's local neighbourhood relationships. Furthermore, the analysis of the complexity of the pixel local connectivity can be approached from fractal analysis, specifically using the LCFD[26], which considers the pixel distribution in terms of local environments.

This study proposes a novel approach that combines skeletonisation, topological descriptors, and LCFD to capture the shape, size, orientation, and connectivity of deforested patches. This approach exploits self-similarity and scaling properties to achieve a more comprehensive characterisation. While previous studies have found a relationship between skeletons and fractals[62], this work represents the first application of this combined approach to characterising deforestation. Our work builds on the paradox of complexity that arises from simplicity[63] to characterise the local connectivity of the deforestation skeleton. We used three binary images of deforested patches from 1990 to 2018 to extract deforestation skeletons. Based on these skeletons, we investigated the potential of pixel neighbourhoods and fractals to identify deforestation hotspots with high spatial connectivity using topological descriptors and LCFD. We applied this analysis to assess the expansion of deforestation in the Sumaco Biosphere Reserve (SBR) in Ecuador, Fig. 1.

Results

Deforestation dynamics at patch and skeleton level

Deforestation in the SBR has followed a dynamic and accelerating trajectory over time, reshaping the landscape in profound ways. Figure 2 illustrates this transformation at both the patch level (Fig. 2a) and the skeleton level (Fig. 2b), providing insight into the evolving spatial structure of deforested areas.

Between 1990 and 2018, deforested patches expanded dramatically from 152 to 1810km^2, illustrating the rapid pace of land cover change. This expansion is mirrored in the extracted skeletons, which capture the underlying connectivity and structural complexity of deforested areas. Over time, these skeletons have grown from 94 km^2 in 1990 to 729 km^2 in 2018, reflecting how isolated clearings have coalesced into larger, more intricate deforested regions.

A detailed analysis of the skeletons from 2005 to 2018 (Fig. 2b) reveals how deforestation patterns have evolved. What were once scattered patches have merged into consolidated deforested zones, creating increasingly

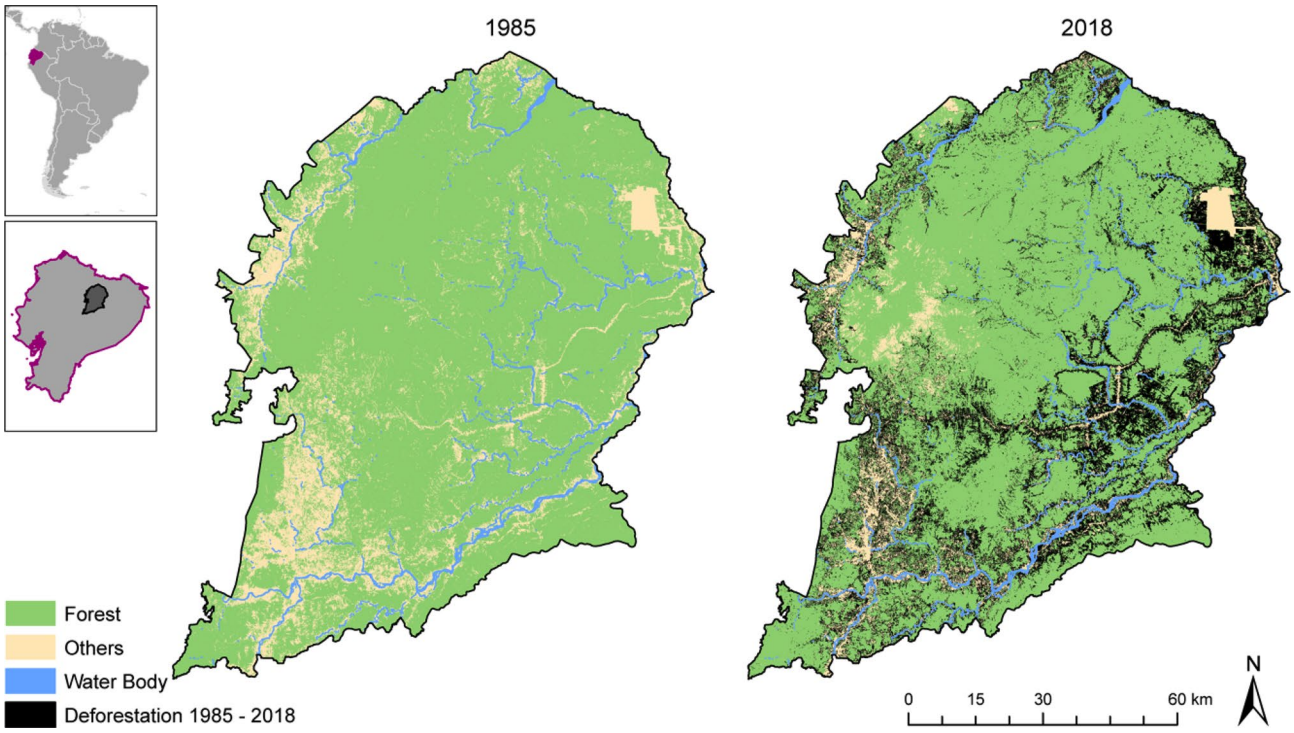

Fig. 1. Sumaco Biosphere Reserve (SBR) located in the headwaters of the Amazon River Basin, showing the extent of native forest in 1985 and forest loss in 2018. The map was created using QGIS[64] version 3.20, https://www.qgis.org/.

complex internal structures. The proportion of the deforested area captured by the skeletons decreased over time, from 62% in 1990 to 44% in 2005 and 40% in 2018. This suggests that as deforestation advances, its structural complexity increases, potentially influencing ecological connectivity and landscape fragmentation.

The skeleton of deforestation metrics

The structural evolution of deforested areas over time is reflected in the changing characteristics of their skeletons. As shown in Fig. 3, the number of skeletons varied significantly across the three time points, reaching its peak in 2005. Compared to 1990, the number of skeletons increased by 204%, before declining by 64% in 2018.

Beyond the overall count, the branching patterns of skeletons reveal important shifts in deforestation structure. In 1990, nearly half (45%) of the skeletons had no branches, indicating a prevalence of small, isolated deforested patches. By 2005, this proportion decreased to 37%, and by 2018, only 32% of skeletons remained unbranched. This shift suggests that deforestation has become increasingly interconnected, forming larger and more complex patterns over time.

Additionally, the skeletons exhibited a growing number of branches, along with increases in both their mean and median lengths. These changes, reflected in rising standard deviation (SD) values, highlight the increasing structural complexity of deforested areas, which is likely indicative of the consolidation of patches and the expansion of clearing activities.

The local connectivity of the skeleton of deforestation

The evolution of deforestation over time is mirrored in the increasing complexity of its spatial structure. Each pixel within the skeletons plays a strategic role in shaping deforestation patterns, as reflected in the topological descriptors summarised in Table 1. These descriptors increased throughout the study period, reflectinghow deforestation progressed through patch expansion and merging, leading to skeletons with increasingly intricate neighbourhood relationships.

At the initial time point, the deforested landscape was characterised by a prevalence of numerous small, isolated patches, with endpoints outnumbering junctions and slabs. As deforestation intensified, previously disconnected patches began to merge, thereby increasing the prominence of slabs and concurrently reducing the proportion of skeletons without branches. By the final time point, this pattern had reversed, with junctions and slabs becoming dominant, while endpoints stabilised, thereby signaling the widespread consolidation of deforested areas.

The complexity of local pixel connections within the skeletons of the SBR is reflected in the differences in LCFD statistical distributions at each time point (Fig. 4). The mean LCFD values for the three time points were 0.69, 0.97, and 1.17, respectively. In particular, the distributions for the two latter time points showed negative skewness. The LCFD spatial distribution of the skeletons (Fig. 5) showed an increase in local complexity over time. At the initial time point, the LCFD was lower, indicating an initial perforation of the forest landscape. The

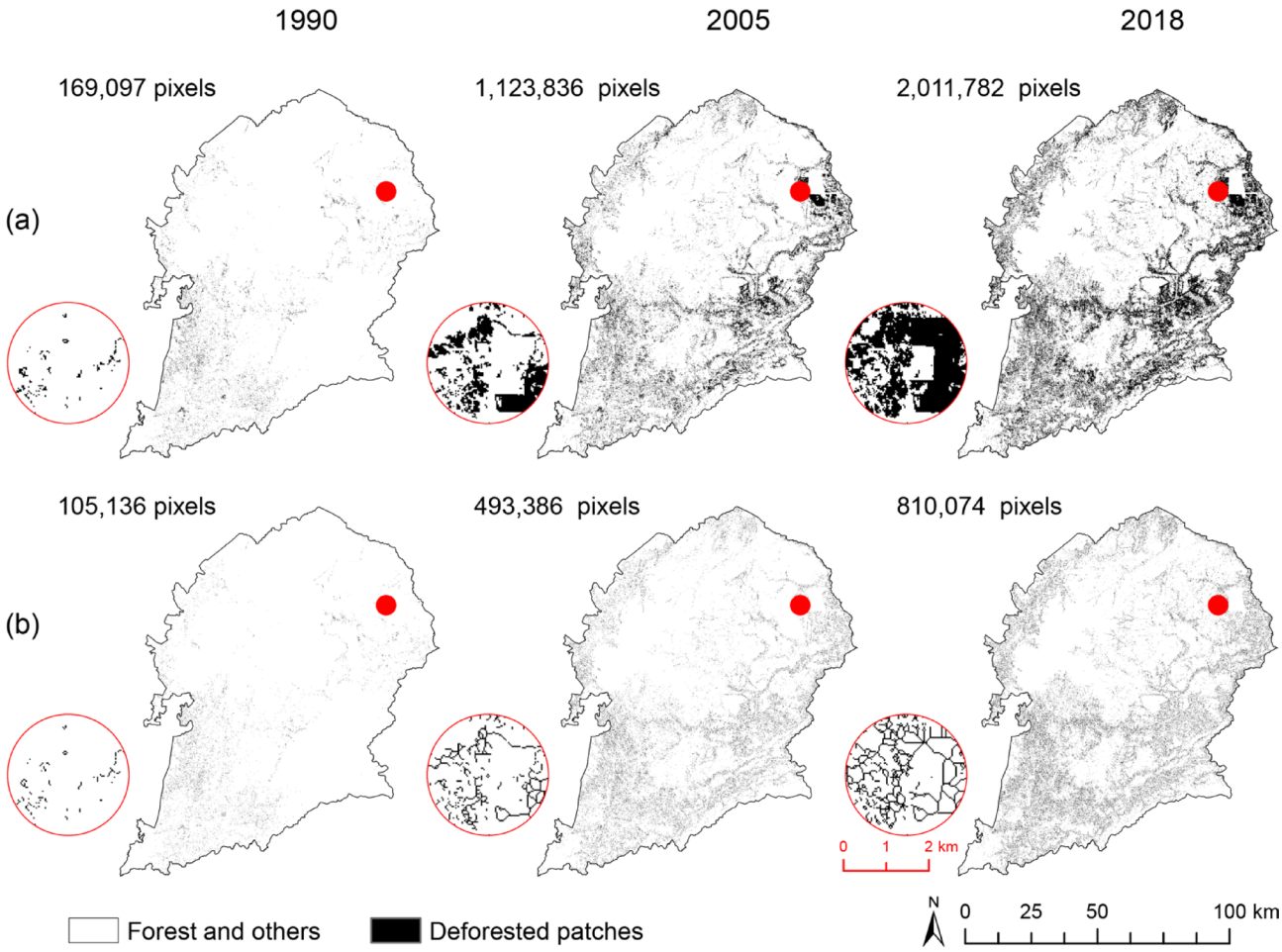

Fig. 2. Binary images of (**a**) deforested patches and (**b**) the skeletons for 1990, 2005 and 2018. Red dots indicate the enlarged area shown in the lower left corner for each year. In the upper left corner, the number of deforested pixels is shown for both the deforested patches and the skeletons. The pixel size is 30 m. The map was created using QGIS[64] version 3.20, https://www.qgis.org/.

subsequent time point showed a consolidation of deforested areas, resulting in an increase in the complexity of local connections.

At the third time point, local pixel connections reached their maximum LCFD values, indicating that the fractal structure of deforestation had enhanced its capacity for expansion. This pattern suggests that the deforested skeletons reinforced their boundaries near forest patches, increasing their capacity to expand further by drawing from adjacent forested areas.

LCFD values (Fig. 5) highlight how spatial complexity evolved across the landscape. Initially, lower LCFD values indicated a perforation phase, where forest loss was scattered and relatively simple in structure. As deforested patches consolidated, the complexity of local connections increased, reaching its peak at the final time point.

The interpretation of LCFD values provides additional insight into these structural changes. Values between 0 and 1 corresponded to isolated skeletons, indicative of early-stage deforestation with low complexity. Conversely, values exceeding 1.00 signified an increase in complexity and greater pixel connectivity, with complexity levels further categorised as medium (≤ 1.34), high (≤ 1.61), and very high (≤ 1.84). To enhance interpretability, forested and deforested patches were included as background, providing a clearer context for the observed patterns.

Mapping deforestation complexity: a composite characterisation

To better understand how deforestation evolves over time, we combined multiple layers of information into a single spatially explicit characterisation. This composite approach (Fig. 6) integrates forest and deforested patches in the background, while skeletons are overlaid with topological descriptors and LCFD categorisation in the foreground. Each skeleton pixel is colour-coded according to its topological properties, and small coloured circles indicate its LCFD category.

In the initial stages of deforestation, small and isolated patches produced simple skeletons, primarily characterised by endpoints and associated with low LCFD values. As deforested areas expanded, skeletons

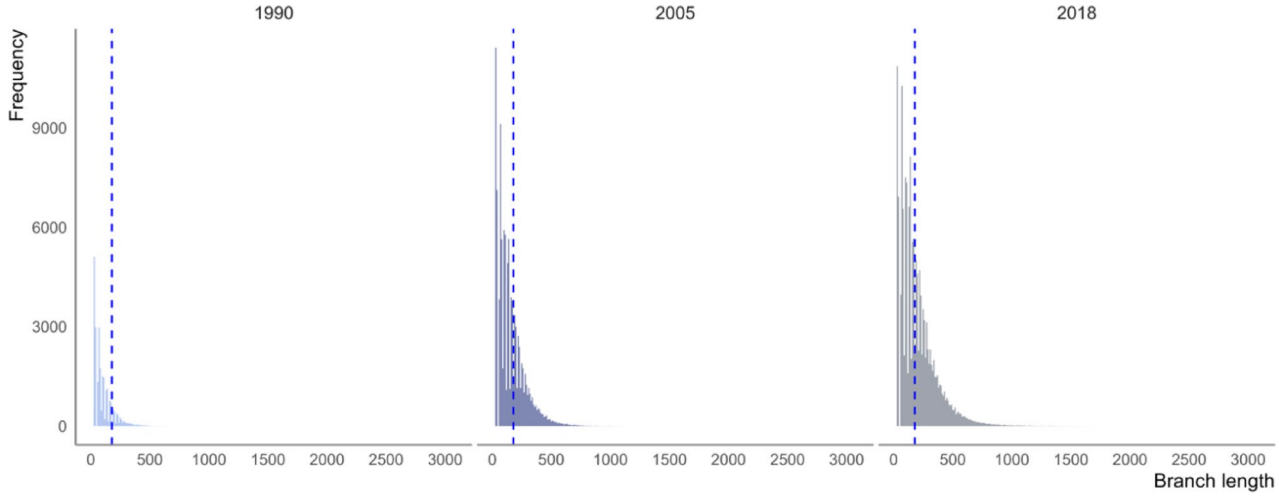

Skeleton metrics	Time points		
	1990	2005	2018
Number of skeletons	32,527	66,362	53,390
Number of skeletons without branches	14,728	24,757	17,015
Total number of branches	25,442	106,122	157,952
Mean branch length (m)	106	158	205
Median branch length	85	127	162
SD of branch length	85	120	162

Fig. 3. Metrics of deforestation skeletons for 1990, 2005, and 2018. The dashed blue line in the distributions at the top represents the mean branch length. Branch length distributions were created using Rstudio[65] version 9.3.

Topological descriptors	Neighbouring pixels	Time points			% Increase	
		1990	2005	2018	(1990–2005)	(2005–2018)
Endpoints	< 2	53,265	133,123	133,582	150%	0.34%
Junctions	> 2	13,592	145,446	331,597	970%	128%
Slabs	= 2	38,279	214,817	344,895	461%	61%

Table 1. Topological descriptors of the deforestation skeletons for 1990, 2005, and 2018.

became more intricate, leading to more complex neighbourhood relationships and higher overall connectivity. This progression is illustrated by the enlarged sections of the SBR in Fig. 6.

In 1990, the configuration of skeletons was relatively simple, dominated by endpoints and slabs with low LCFD values. By 2005, the pattern shifted as deforestation intensified, with skeletons characterised by an increased presence of slabs and junctions exhibiting medium and high LCFD values. In 2018, the skeletons displayed a dominance of junctions, with very high LCFD values marking the most structurally complex deforested regions.

Although both LCFD values and topological descriptors reflect deforestation complexity, they do not have a direct linear relationship. LCFD values depend on the sampling window surrounding each pixel, thereby capturing the connectivity within its local neighbourhood. In contrast, topological descriptors classify skeleton pixels based only on the neighbouring pixels, making them independent of the overall skeleton geometry. This approach complements conventional methods for spatially prioritising reforestation pathways by integrating structural connectivity (topological descriptors) and local complexity (LCFD), providing a more detailed and spatially explicit understanding of deforestation patterns.

Prioritising reforestation efforts: Interpreting skeleton complexity

Understanding the spatial arrangement of skeleton pixels can facilitate the prioritisation of reforestation initiatives. The priority ranking is based on the potential impact of each structure on deforestation dynamics, taking into account both its topological role and its LCFD value.

- Junctions play a critical role in connectivity, and those with high LCFD represent active deforestation hot-spots, warranting the highest priority.

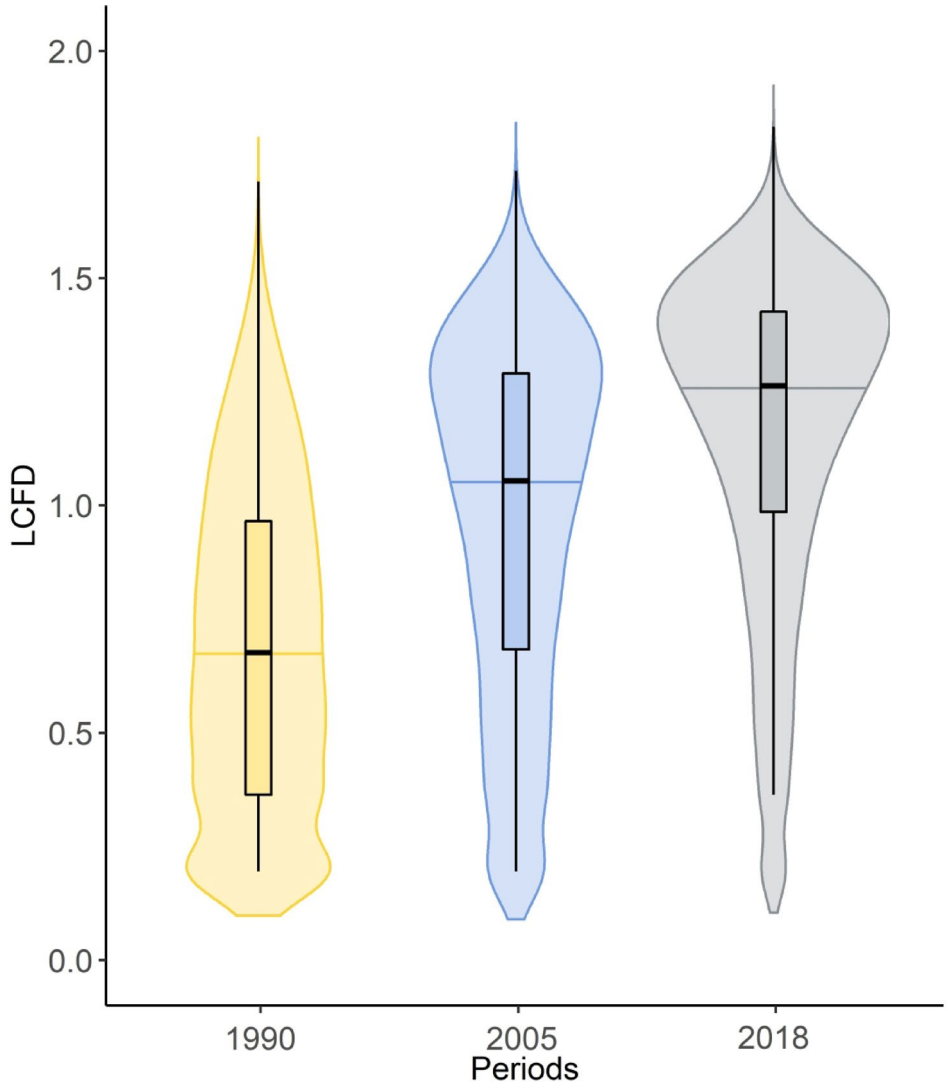

Fig. 4. Statistical distribution of local connected fractal dimension (LCFD) values of skeletons for 1990, 2005, and 2018. Distribution graphs were created using Rstudio[65] version 9.3.

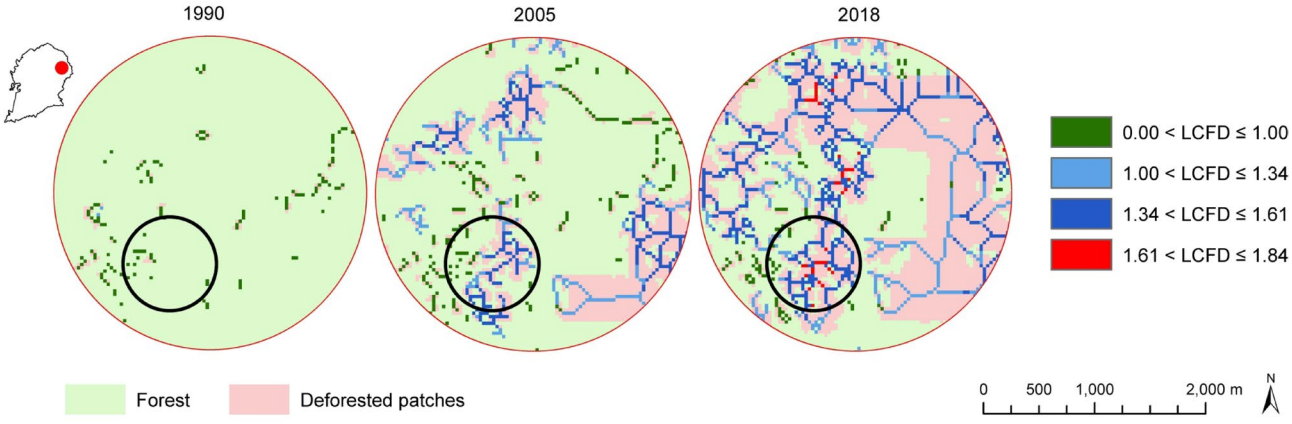

Fig. 5. Spatial distribution of deforestation skeletons by Local Connected Fractal Dimensions (LCFD), colour-coded using K-means. The circle is located in the *Sumaco* Biosphere Reserve (SBR) and shown for each year of analysis. Black circles are enlarged and detailed in Fig. 6. The map was created using QGIS[64] version 3.20, https://www.qgis.org/.

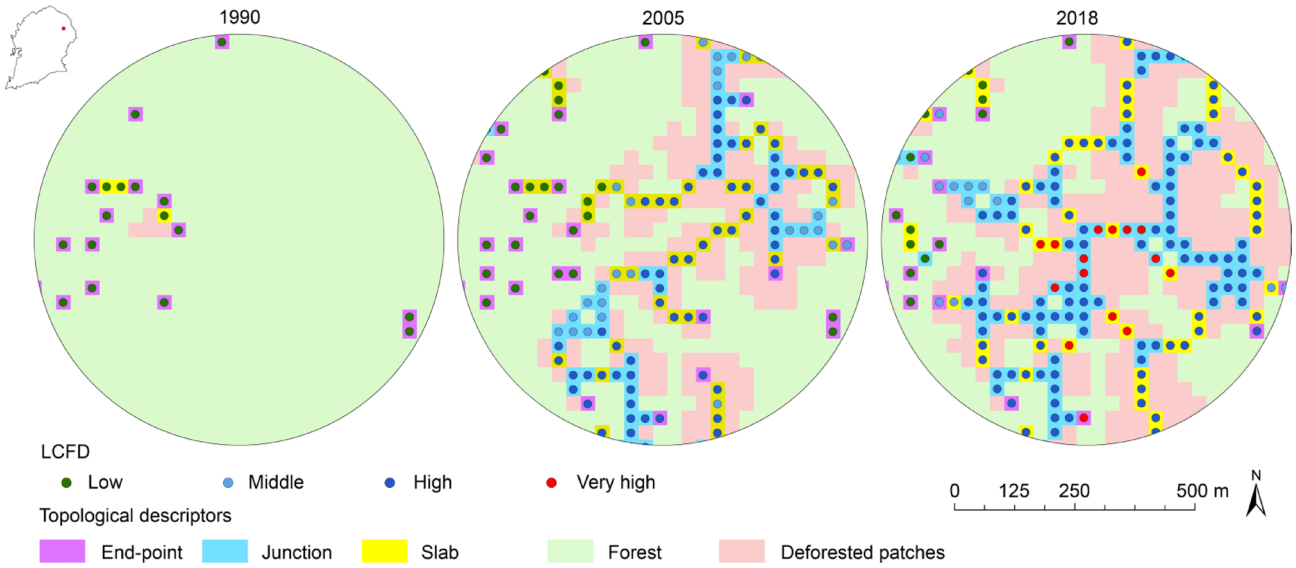

Fig. 6. Spatially explicit characterisation of the deforestation skeleton using Local Connected Fractal Dimensions (LCFD) and topological descriptors. The circle is located in the Sumaco biosphere reserve (SBR). This view is an enlarged area of Fig. 5. The map was created using QGIS[64] version 3.20, https://www.qgis.org/.

- Slabs with high LCFD indicate areas of ongoing deforestation that could be strategically disrupted, while those with moderate LCFD require monitoring due to their potential transition to higher activity.
- Endpoints with high LCFD may seem less significant but are highly sensitive to neighbourhood changes, meaning that even minor expansions can disproportionately increase the complexity of deforestation.

Different combinations of LCFD categories and topological descriptors indicate varying levels of concern, with the following cases ranked in increasing order of urgency:

- A junction (light blue pixel) with high LCFD (red dot) represents an active deforestation hotspot where multiple branches converge, making it a key structural connector. These pixels require urgent attention as they have the highest potential for further deforestation expansion. (Priority Level 1)
- A slab (yellow pixel) with high LCFD (red dot) is an active spot that could be targeted for intervention to disrupt deforestation patterns. (Priority Level 2)
- A slab (yellow pixel) with moderate LCFD (green dot) is a point that should be continuously monitored, as it may transition to a more active state. (Priority Level 3)
- A junction (light blue pixel) with moderate LCFD (green dot) is a low-complexity point that requires less immediate concern but still merits monitoring. (Priority Level 4)
- An endpoint (magenta pixel) with high LCFD (red dot) represents an active deforestation endpoint that, while seemingly minor, is highly sensitive to neighbourhood changes. Even minor expansions in surrounding pixels could substantially increase the overall deforestation complexity. (Priority Level 5)

Additionally, two cases are structurally impossible:

- An endpoint (magenta pixel) with low LCFD (blue dot) in an isolated skeleton of one or two pixels.
- An endpoint (magenta pixel) with high LCFD (red dot) in an isolated skeleton of one or two pixels.

Owing to the dynamic nature of the analysis, the skeletons in our study vary their original structure once additional deforested areas have altered the boundary shapes. While the structure is maintained in some instances, in most cases, it undergoes changes. This variability necessitates the implementation of a dynamic approach when calculating the percentage of junctions with high LCFD values that subsequently expanded the deforested area. The skeleton structure can shift slightly between stages, with the displacement typically confined to one or two pixels around the previously identified high LCFD junction. This highlights the necessity for prompt action, as such changes in the skeleton can compromise the accuracy of the analysis if not addressed in a timely manner.

This framework provides a structured approach to identifying critical intervention points within deforestation networks. By leveraging both topological descriptors and LCFD categories, this method offers a novel perspective for prioritising reforestation pathways and mitigating deforestation expansion in a spatially informed manner.

Discussion

The proposed method allowed the characterisation of deforestation connectivity and expansion patterns at the skeleton level. The method captured the complete geometry of each deforested patch by incorporating it into a

skeleton representation. LCFD and topological descriptors are then applied to this skeleton. Our method differs from other spatial metrics such as Moran's I[66–68], conventional landscape ecology metrics[69,70], density maps and heat maps. The strengths are (i) the nature of the analysis which is cell-based, (ii) the robustness of the statistical sampling through a moving window[71], (iii) the window scale sampling to account for neighbourhood connectivity, (iv) the scale or extent invariance due to the fractal nature of deforestation[26], and iv) the absence of spatial correlation with other variables. The latter is a common limitation of conventional spatial metrics in the analysis of deforestation.

The applicability of the skeleton analysis was tested in the SBR, which is a representative site in the upper Amazon basin with high deforestation rates[72–74] and complex spatial patterns[75]. In addition, this Biosphere Reserve shows high potential areas for effective reforestation[76] as a model site for large-scale forest restoration in the Amazon. Three time points have been used to illustrate the expansion of deforestation. The difference between them is not homogeneous, as the analysis was carried out considering the availability of data and the year in which extensive agriculture was promoted in Ecuador.

The increase in LCFD from 1990 to 2018 was motivated by an accelerated expansion of the agricultural boundary, which was stimulated by government policy in 2000. This period was well known in Ecuador as the "inclusive agriculture" and "inclusive business" programs, financed by public and private institutions[77]. From this point onwards, the LCFD increased in a similar way to the increase in the number of skeleton branches (Fig. 3). Both corresponded to a remarkable increase in the number of topological descriptors, especially in the junctions and slabs (Table 1). The number of skeletons decreased from 2005 to 2018 due to attrition and shrinkage land processes. At the same time, the mean length of the skeleton branches increased, reflecting the potential of deforestation expansion structures because of the increasing number of endpoints with 150% in 2005 (Table 1). However, it was not only an increase of endpoints that was associated with an increase in LCFD complexity. From 2005 to 2018, the endpoints remained stable, and junctions and slabs increased, implying that the structural pattern of deforestation was strengthened by increasing the skeleton branching and also by increasing internal connectivity.

The analysis of topological descriptors (Table 1) reveals distinct trends in deforestation dynamics. The number of junctions exhibited the highest rate of increase (970% from 1990 to 2005 and 128% from 2005 to 2018), followed by slabs, while endpoints stabilised after an initial rise. This pattern suggests a transition from early fragmentation to increased connectivity in deforested areas over time. The spatial morphology of deforested patches further supports this structured progression. Skeleton analysis indicates that deforestation follows a complex spatial process interaction, with patches perforating, dissecting, fragmenting, shrinking, and merging in the landscape rather than being randomly distributed. The configuration of the skeletons highlights the formation of concentrated areas of deforestation, reflecting land-use decisions and spatial dependencies. The fractal nature of deforestation patterns underscores the influence of hierarchical organization, demonstrating that deforestation is not a purely stochastic phenomenon but a complex landscape process that evolves across multiple scales.

The composite characterisation for deforestation hotspots included the LCFD results and the topological descriptors of the skeletons (Fig. 6). Both allowed to simultaneously categorise the complexity of pixel connectivity and neighbourhood relationships. This is crucial for prioritising areas that can be considered for reforestation pathways that progressively contribute to the recovery of forest landscape connectivity. There is no direct relationship between LCFD values and topological descriptors of the skeleton, as it depends on the spatial arrangement of the skeletons and branches at the local scale. Therefore, coloured dots were used to identify the LCFD value range for each topological descriptor represented in each pixel of the skeleton.

Although this spatially explicit characterisation was developed to characterise the skeleton of deforestation, it is also valuable for representing the structure of any transformed landscape. Coloured dots for the LCFD and contrasting coloured pixels for the topological descriptors provided a quick and reliable tool for identifying the local complexity connectivity. This graphical characterisation of the structure can be applied to landscape modelling and route planning, such as reforestation corridors, as the results are georeferenced.

Successful ecosystem restoration takes into account ecological, economic, and social needs. Prior to implementing a restoration project or commencing restoration activities, a restoration assessment is mandatory. In the context of assessing forest restoration among a range of requirements, there is a need to provide a spatially explicit prioritisation of restoration across spatial scales[78]. Our work contributes to this requirement by providing a spatially explicit prioritisation tool based on the pixel categorisation of the basic structure of the deforested patch, the skeleton. This enables for identifying local hot spots that may be considered in fund investment programs for reforestation.

Reforestation funds are usually small and expectations of reforestation targets are high. Therefore, regardless of scale, reforestation is challenging in terms of prioritisation. A scale invariant spatial prioritisation is required to reforest as much as possible and ensure the long-term sustainability of forest patches at the landscape scale. Our work offers the possibility to define localised restoration actions in an area smaller than a patch through the skeleton. Through pixel categorisation based on LCFD, it is possible to maintain an invariant spatial prioritisation due to the self-similarity property of fractal objects. This pixel categorisation is also supported by topological descriptors.

A common goal in scenario definition and decision-making is to achieve connectivity in forest landscapes while halting deforestation. Behind this goal, there are a large number of factors and actors involved with different opinions, adding complexity to restoration initiatives. Although social discrepancies are not considered in this work, the results presented here could inspire the next deforestation strategies that also include social and economic criteria to regulate smart reforestation worldwide.

While the method provides a novel approach to characterising deforestation connectivity and expansion patterns, certain limitations should be acknowledged. First, the computational cost of calculating LCFD in

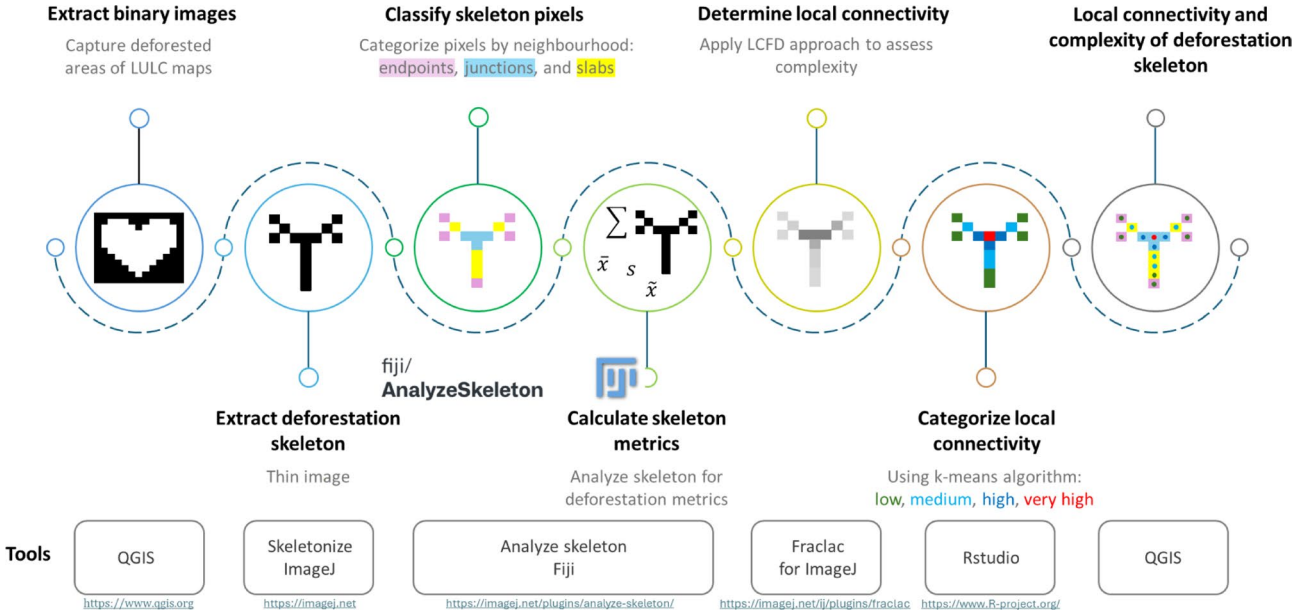

Fig. 7. Methodology workflow. The diagram was created in Microsoft PowerPoint 365 using ImageJ (version 1.54 h). The outputs are an example of heart image analysis.

large areas is significant, requiring extensive processing time and limiting scalability. Furthermore, there is no single, direct computational framework to perform all calculations in a comprehensive manner. Instead, several intermediate steps require human intervention, particularly during the georeferencing process between ImageJ and GIS software, which requires user intervention and consequently slows down the processing. Second, the approach does not account for land-use constraints within the analysed area. Certain landscapes, such as urban areas, transportation infrastructure, and dams, are unlikely to revert to forest cover, which affects the feasibility of restoration planning. Furthermore, while the methodology provides a spatially explicit framework for deforestation prioritisation, a broader discussion with stakeholders is essential to ensure its practical implementation. Incorporating local perspectives and socio-economic considerations could enrich the applicability of composite LCFD analysis and topological descriptor-based prioritisation. Future research could focus on automating key computational processes, integrating machine learning for predictive modelling, and expanding the framework to consider socio-economic and institutional factors that influence deforestation and restoration potential. Additionally, exploring the interaction between LCFD and other ecological indicators, such as habitat fragmentation and biodiversity loss, could provide a more holistic understanding of landscape transformation and improve conservation strategies.

Methods

Case study

The SBR was chosen as a case study because it is considered to be one of the most biodiverse and culturally rich areas on the planet[79], while at the same time being heavily impacted by human activities such as agriculture and livestock expansion[68]. The SBR contains a variety of drivers of deforestation in the Amazon region, making it an excellent location to investigate the impacts of land cover change, such as deforestation. Previous studies confirm the importance of the site in terms of ecosystem services[80], biodiversity[81], livelihoods[82], carbon sequestration[83], and traditional agricultural systems[74]. The Amazon region has undergone enormous landscape changes over the last three decades. However, the environmental impacts are more concerning when considering the ecological sensitivity of the headwaters of the Amazon River basin where SBR is located (Fig. 1). The SBR preserves extensive, intact, tropical humid forest, which is a hotspot for conservation and restoration. For the analysis, the entire SBR was considered without zoning to avoid truncating the deforested areas.

Skeleton of deforestation analysis

Extracting skeletons of deforestation and metrics

The binary images of deforested patches were used as input to obtain the deforestation skeleton, Fig. 7. These images were extracted by LULC change analysis, using QGIS (version 3.20, https://www.qgis.org/), between map pairs from the MAPBIOMAS project in 1990, 2005, and 2018 to analyse the expansion of deforestation five years before and after the promotion of "inclusive agriculture" and "inclusive business" programs, and its expansion until 2018. The MAPBIOMAS map set was developed based on LULC maps from the Ministry of Environment, Water and Ecological Transition of Ecuador, which were used to train classification algorithms and evaluate the quality of image classification[84,85]. The change from forest to agricultural land or urbanisation was referred to as deforestation.

The skeleton of deforestation was extracted using ImageJ software (version 1.54 h, https://imagej.net/)[86], which applied a 1-pixel-width parallel thinning algorithm[87] with a pixel resolution of 30 m. Each binary image of the skeletons contained values of 0 and 1, representing background and deforested pixels, respectively. The quantification of the skeletons and branches was followed by the calculation of topological descriptors to classify the skeleton pixels into three categories: endpoints, junctions, and slabs. This classification was based on the number of neighbouring pixels within the connectivity framework used by the AnalyzeSkeleton tool (version 3.4.2, https://imagej.net/plugins/analyze-skeleton/)[88]. See Fig. S1 online in the supplementary information for a detailed overview of the process followed and the open-source tools used to perform the analysis.

In 2D images, the algorithm employs an 8-connected neighbourhood system. Accordingly, endpoints are defined as pixels with fewer than two neighbours, junctions as those with more than two neighbours, and slabs as those with exactly two neighbouring pixels. Skeleton metrics and topological descriptors were calculated for each time point in the analysis.

Local connected fractal dimension of skeletons

The local complexity of skeleton pixel connections was performed using the LCFD approach[89] from FracLac (version 2.5, https://imagej.net/ij/plugins/fraclac/FLHelp/t4.htm), Fig. 7. We categorised the LCFD values using the unsupervised K-means algorithm, using stats package of R (version 4.3.2, https://R-project.org/)[90], to obtain four complexity thresholds of skeletons. Every threshold range was colour coded. The LCFD was calculated by the linear regression of the logarithm of the mass (pixels), (ε) in a box of size ε on the logarithm of ε. This scaling relation is expressed in the following equation:

$$LCFD = \frac{\log\left[M\left(\varepsilon\right)\right]}{\log\varepsilon}$$

where $M\left(\varepsilon\right)$ is the number of locally connected pixels (eight-neighbourhood connection) in a box of side size ε[89]. From Eq. 1, the LCFD = 2 if the object is completely filled, and therefore the object is two-dimensional. On the other hand, if the object is a straight line (one-dimensional), then the LCFD = 1. The LCFD results are more useful for values in the range $1.0 < \text{LCFD} \leq 2.00$, as these describe the local complexity of the set.

Data availability

The datasets used and/or analysed during the current study are available from Zenodo (https://zenodo.org/records/14841710). These data are provided for non-commercial purposes only. If you use this dataset for research, please be sure to cite this paper.

Received: 26 July 2024; Accepted: 16 May 2025
Published online: 25 May 2025

References

1. Pendrill, F. et al. Disentangling the numbers behind agriculture-driven tropical deforestation. *Science* **377**, eabm9267 (2022).
2. Meng, Z. et al. Post-2020 biodiversity framework challenged by cropland expansion in protected areas. *Nat. Sustain.* **6**, 758–768 (2023).
3. Seto, K. C. & Ramankutty, N. Hidden linkages between urbanization and food systems. *Science* **352**, 943–945 (2016).
4. Santos, Y. L. F. et al. Amazon deforestation and urban expansion: simulating future growth in the Manaus metropolitan region, Brazil. *J. Environ. Manag.* **304**, 114279 (2022).
5. Brandão, F., Befani, B., Soares-Filho, J., Rajão, R. & Garcia, E. How to halt deforestation in the Amazon? A bayesian process-tracing approach. *Land. Use Policy* **133**, 106866 (2023).
6. de Oliveira, G. et al. Increasing wildfires threaten progress on halting deforestation in Brazilian Amazonia. *Nat. Ecol. Evol.* **7**, 1945–1946 (2023).
7. Mondal, P., McDermid, S. S. & Qadir, A. A reporting framework for sustainable development goal 15: Multi-scale monitoring of forest degradation using MODIS, landsat and sentinel data. *Remote Sens. Environ.* **237**, 111592 (2020).
8. Huan, Y. & Zhu, X. Interactions among sustainable development goal 15 (life on land) and other sustainable development goals: Knowledge for identifying global conservation actions. *Sustain. Dev.* **31**, 321–333 (2023).
9. Flores, B. M. et al. Critical transitions in the Amazon forest system. *Nature* **626**, 555–564 (2024).
10. Boers, N., Marwan, N., Barbosa, H. M. J. & Kurths, J. A deforestation-induced tipping point for the South American monsoon system. *Sci. Rep.* **7**, 41489 (2017).
11. Seydewitz, T., Pradhan, P., Landholm, D. M. & Kropp, J. P. Deforestation drivers across the tropics and their impacts on carbon stocks and ecosystem services. *Anthr Sci.* **2**, 81–92 (2023).
12. Andrieu, E., Ladet, S., Heintz, W. & Deconchat, M. History and spatial complexity of deforestation and logging in small private forests. *Landsc. Urban Plan.* **103**, 109–117 (2011).
13. Solé, R. & Bascompte, J. *Self-Organization in Complex ecosystems.(MPB-42)* vol. 58 (Princeton University Press, 2012).
14. Kleemann, J., Baysal, G., Bulley, H. N. N. & Fürst, C. Assessing driving forces of land use and land cover change by a mixed-method approach in north-eastern Ghana, West Africa. *J. Environ. Manag.* **196**, 411–442 (2017).
15. Rueda, X., Velez, M. A., Moros, L. & Rodriguez, L. A. Beyond proximate and distal causes of land-use change: Linking individual motivations to deforestation in rural contexts. *Ecol. Soc.* **24**(1), 4 (2019).
16. Alves, M. T. R. et al. Effects of settlement designs on deforestation and fragmentation in the Brazilian Amazon. *Land. Use Policy* **109**, 105710 (2021).
17. Arima, E. Y., Walker, R. T., Perz, S. & Souza, C. Jr. Explaining the fragmentation in the Brazilian Amazonian forest. *J. Land. Use Sci.* **11**, 257–277 (2016).
18. Biggs, T. W., Dunne, T., Roberts, D. A. & Matricardi, E. The rate and extent of deforestation in watersheds of the Southwestern Amazon basin. *Ecol. Appl.* **18**, 31–48 (2008).
19. Wolfersberger, J., Amacher, G. S., Delacote, P. & Dragicevic, A. The dynamics of deforestation and reforestation in a developing economy. *Environ. Dev. Econ.* **27**, 272–293 (2022).
20. Sandker, M., Finegold, Y., D'Annunzio, R. & Lindquist, E. Global deforestation patterns: Comparing recent and past forest loss processes through a spatially explicit analysis. *Int. Rev.* **19**, 350–368 (2017).

21. Antwi, E. K. et al. A global review of cumulative effects assessments of disturbances on forest ecosystems. *J. Environ. Manag.* **317**, 115277 (2022).
22. Fitzsimmons, M. Effects of deforestation and reforestation on landscape Spatial structure in boreal Saskatchewan, Canada. *Ecol. Manag.* **174**, 577–592 (2003).
23. McGarigal, K. & Marks, B. J. FRAGSTATS: Spatial pattern analysis program for quantifying landscape structure. https://doi.org/10.2737/pnw-gtr-351 (1995) (1995).
24. Forman, R. T. T. Some general principles of landscape and regional ecology. *Landsc. Ecol.* **10**, 133–142 (1995).
25. Forman, R. T. T. *Land Mosaics: The Ecology of Landscapes and Regions* (Cambridge Cambridge University, 1995).
26. Urgilez-Clavijo, A., Rivas-Tabares, D. A. & Martín-Sotoca, J. J. & Tarquis Alfonso, A. M. Local fractal connections to characterize the spatial processes of deforestation in the Ecuadorian Amazon. *Entropy* **23**(6) (2021).
27. Ma, Y. et al. The deforestation and biodiversity risks of power plant projects in Southeast Asia: A big data spatial analytical framework. *Sustainability* **15**(19) (2023).
28. Soille, P. & Vogt, P. Morphological Spatial pattern analysis: Open source release. *Int. Arch. Photogramm Remote Sens. Spat. Inf. Sci.* **XLVIII-4/W**, 427–433 (2022).
29. Rivas, C. A., Guerrero-Casado, J. & Navarro-Cerrillo, R. M. Functional connectivity across dominant forest ecosystems in Ecuador: A major challenge for a country with a high deforestation rate. *J. Nat. Conserv.* **78**, 126549 (2024).
30. Ma, J., Li, J., Wu, W. & Liu, J. Global forest fragmentation change from 2000 to 2020. *Nat. Commun.* **14**, 3752 (2023).
31. Montibeller, B., Kmoch, A., Virro, H., Mander, Ü. & Uuemaa, E. Increasing fragmentation of forest cover in Brazil's legal Amazon from 2001 to 2017. *Sci. Rep.* **10**, 5803 (2020).
32. Peptenatu, D. et al. A new fractal index to classify forest fragmentation and disorder. *Landsc. Ecol.* **38**, 1373–1393 (2023).
33. Andronache, I. et al. Dynamics of forest fragmentation and connectivity using particle and fractal analysis. *Sci. Rep.* **9**, 12228 (2019).
34. Andronache, I. Analysis of forest fragmentation and connectivity using fractal dimension and succolarity. *Land* **13**(2) (2024).
35. Nunes, S. et al. Challenges and opportunities for large-scale reforestation in the Eastern Amazon using native species. *Ecol. Manage.* **466**, 118120 (2020).
36. Gastauer, M., Cavalcante, R. B. L., Caldeira, C. F. & de Nunes, S. S. Structural hurdles to large-scale forest restoration in the Brazilian Amazon. *Front Ecol. Evol* **8** (2020).
37. Erbaugh, J. T. et al. Global forest restoration and the importance of prioritizing local communities. *Nat. Ecol. Evol.* **4**, 1472–1476 (2020).
38. Ortega Adarme, M., Doblas Prieto, J., Queiroz Feitosa, R. & De Almeida, C. A. Improving deforestation detection on tropical rainforests using Sentinel-1 data and convolutional neural networks. *Remote Sens.* **14**(14), (2022).
39. Cai, Y., Shi, Q., Xu, X. & Liu, X. A novel approach towards continuous monitoring of forest change dynamics in fragmented landscapes using time series landsat imagery. *Int. J. Appl. Earth Obs Geoinf.* **118**, 103226 (2023).
40. Fassnacht, F. E., White, J. C., Wulder, M. A. & Næsset, E. Remote sensing in forestry: Current challenges, considerations and directions. *Int. J. Res.* **97**, 11–37 (2024).
41. Wang, Z. et al. Change detection on high-resolution remote sensing imagery with scribble interaction. *Int. J. Appl. Earth Obs Geoinf.* **128**, 103761 (2024).
42. Wang, Z. et al. SiamHRnet-OCR: A novel deforestation detection model with high-resolution imagery and deep learning. *Remote Sens.* **15**, (2023).
43. DeValue, K. et al. *Halting Deforestation from Agricultural Value Chains: the Role of Governments* (FAO, 2021).
44. Hänggli, A. et al. A systematic comparison of deforestation drivers and policy effectiveness across the Amazon biome. *Environ. Res. Lett.* **18**, 73001 (2023).
45. Soille, P. & Vogt, P. Morphological segmentation of binary patterns. *Pattern Recognit. Lett.* **30**, 456–459 (2009).
46. Beisbart, C., Buchert, T. & Wagner, H. Morphometry of spatial patterns. *Phys. Stat. Mech. Its Appl.* **293**, 592–604 (2001).
47. Nowosad, J. Motif: an open-source R tool for pattern-based spatial analysis. *Landsc. Ecol.* **36**, 29–43 (2021).
48. Simonetti, D., Marelli, A. & Eva, H. *IMPACT – Portable GIS Toolbox for Image Processing and Land Cover Mapping* (Publications Office of the European Union, 2015). https://doi.org/10.2788/143497
49. Wang, H. et al. Spatial-temporal pattern analysis of landscape ecological risk assessment based on land use/land cover change in Baishuijiang National nature reserve in Gansu Province, China. *Ecol. Indic.* **124**, 107454 (2021).
50. John, A. M., Elfanagely, O., Ayala, C. A., Cohen, M. & Prestigiacomo, C. J. The utility of fractal analysis in clinical neuroscience. **26**, 633–645 (2015).
51. Duan, Q. et al. Review about the application of fractal theory in the research of packaging materials. *Materials* **14** (2021).
52. Li, M. et al. Comprehensive 3D phenotyping reveals continuous morphological variation across genetically diverse sorghum inflorescences. *New. Phytol.* **226**, 1873–1885 (2020).
53. Frankhauser, P. & Pumain, D. Fractals and geography. *Mach. Learn. City* 31–55. https://doi.org/10.1002/9781119815075.ch3 (2022).
54. Martinez, F., Manriquez, H., Ojeda, A. & Olea, G. Organization patterns of complex river networks in Chile: A fractal morphology. *Mathematics* **10** (2022).
55. Shit, P. K., Bhunia, G. S. & Maiti, R. Soil crack morphology analysis using image processing techniques. *Model. Earth Syst. Environ.* **1**, 35 (2015).
56. Ren, J., Xie, R., Zhu, H., Zhao, Y. & Zhang, Z. Comparative study on the abilities of different crack parameters to estimate the salinity of soda saline-alkali soil in Songnen plain, China. *CATENA* **213**, 106221 (2022).
57. James, P. M. A. & Fortin, M. J. Ecosystems and Spatial patterns. in *Encyclopedia of Sustainability Science and Technology* (ed Meyers, R. A.) 3326–3342 (Springer, 2012). https://doi.org/10.1007/978-1-4419-0851-3_227.
58. Ayzenberg, V. & Lourenco, S. F. Skeletal descriptions of shape provide unique perceptual information for object recognition. *Sci. Rep.* **9**, 9359 (2019).
59. Thomas, R. D. K. & Reif, W. E. The skeleton space: A finite set of organic designs. *Evolution (N Y)* **47**, 341–360 (1993).
60. Haddad, N. M. et al. Habitat fragmentation and its lasting impact on Earth's ecosystems. *Sci. Adv.* **1**, e1500052 (2025).
61. Wang, Z. et al. Biodiversity conservation in the context of climate change: Facing challenges and management strategies. *Sci. Total Environ.* **937**, 173377 (2024).
62. Sagar, B. S. D. Fractal relation of a morphological skeleton. *Chaos Solitons Fractals* **7**, 1871–1879 (1996).
63. Bunge, M. The complexity of simplicity. *J. Philos.* **59**, 113–135 (1962).
64. QGIS.org. QGIS Geographic Information System. Open Source Geospatial Foundation Project. (2023).
65. RStudio Team. RStudio: Integrated Development Environment for R. (2023).
66. Castro-Nunez, A. C., Villarino, M. E. J., Bax, V., Ganzenmüller, R. & Francesconi, W. Broadening the perspective of zero-deforestation interventions in Peru by incorporating concepts from the global value chain literature. *Sustainability* **13**(21) (2021).
67. Anselin, L. Local indicators of spatial association—LISA. *Geogr. Anal.* **27**, 93–115 (1995).
68. Ferrer Velasco, R., Köthke, M., Lippe, M. & Günter, S. Scale and context dependency of deforestation drivers: Insights from spatial econometrics in the tropics. *PLoS One* **15**, e0226830 (2020).
69. Mansori, M., Badehian, Z., Ghobadi, M. & Maleknia, R. Assessing the environmental destruction in forest ecosystems using landscape metrics and spatial analysis. *Sci. Rep.* **13**, 15165 (2023).
70. San-José, M. et al. Effects of landscape structure on restoration success in tropical premontane forest. *Sci. Rep.* **12**, 13452 (2022).

71. Cheng, Q. The gliding box method for multifractal modeling. *Comput. Geosci.* **25**, 1073–1079 (1999).
72. Long, B. Conflicting land-use schemes in the Ecuadorian Amazon: The case of Sumaco. *Geography* **77**, 336–348 (1992).
73. Urgilez-Clavijo, A., de la Riva, J., Rivas-Tabares, D. A. & Tarquis, A. M. Linking deforestation patterns to soil types: A multifractal approach. *Eur. J. Soil. Sci.* **72**, 635–655 (2021).
74. Torres, B., Vasco, C., Günter, S. & Knoke, T. Determinants of agricultural diversification in a hotspot area: Evidence from colonist and indigenous communities in the Sumaco biosphere reserve, Ecuadorian Amazon. *Sustainability* **10**(5) (2018).
75. Geist, H. J. & Lambin, E. F. Proximate causes and underlying driving forces of tropical deforestation: Tropical forests are disappearing as the result of many pressures, both local and regional, acting in various combinations in different geographical locations. *Bioscience* **52**, 143–150 (2002).
76. der Hoek, Y. The potential of protected areas to halt deforestation in Ecuador. *Environ. Conserv.* **44**, 124–130 (2017).
77. Kovacic, Z. & Viteri Salazar, O. The lose-lose predicament of deforestation through subsistence farming: unpacking agricultural expansion in the Ecuadorian Amazon. *J. Rural Stud.* **51**, 105–114 (2017).
78. DellaSala, D. A. et al. A citizen's call for ecological forest restoration: forest restoration principles and criteria. *Ecol. Restor.* **21**, 14 LP – 23 (2003).
79. Myers, N. Threatened biotas: Hot spots in tropical forests. *Environmentalist* **8**, 187–208 (1988).
80. Delgado-Aguilar, M. J., Konold, W. & Schmitt, C. B. Community mapping of ecosystem services in tropical rainforest of Ecuador. *Ecol. Indic.* **73**, 460–471 (2017).
81. Torres, B., Herrera-Feijoo, R. J., Torres-Navarrete, A., Bravo, C. & García, A. Tree diversity and its ecological importance value in silvopastoral systems: A study along elevational gradients in the Sumaco biosphere reserve, Ecuadorian Amazon. *Land* **13**(3) (2024).
82. Torres, B. et al. Productive livestock characterization and recommendations for good practices focused on the achievement of the SDGs in the Ecuadorian Amazon. *Sustainability* **14**(17) (2022).
83. Torres, B. et al. Carbon stock assessment in silvopastoral systems along an elevational gradient: A study from cattle producers in the Sumaco biosphere reserve, Ecuadorian Amazon. *Sustainability* **15**(1) (2023).
84. Souza, C. & Azevedo, T. *MapBiomas General Handbook* (MapBiomas, São Paulo, Brazil, 2017).
85. Borja, M. O. & Aguilar, C. W. H. & C. J. *Documento de bases teóricas de algoritmo (ATBD) MapBiomas Amazonía colección 4.0, apéndice Ecuador - colección 4.0 de mapas anuales de cobertura y uso del suelo de la Amazonía* (2022).
86. Karperien, A. *Fraclac for ImageJ* (Charles Sturt University, 2013).
87. Lee, T. C., Kashyap, R. L. & Chu, C. N. Building skeleton models via 3-D medial surface axis thinning algorithms. *CVGIP Graph Model. Image Process.* **56**, 462–478 (1994).
88. Arganda-Carreras, I., Fernández-González, R. & Muñoz-Barrutia, A. 3D reconstruction of histological sections: application to mammary gland tissue. *Microsc Res. Tech.* **73**, 1019–1029 (2010).
89. Landini, G., Murray, P. I. & Misson, G. P. Local connected fractal dimensions and lacunarity analyses of 60 degrees fluorescein angiograms. *Invest. Ophthalmol. Vis. Sci.* **36**, 2749–2755 (1995).
90. R Core Team. R: A language and environment for statistical computing. (Foundation for Statistical Computing, Vienna, Austria, 2013).

Acknowledgements

The first author acknowledges support from Universidad del Azuay through the project "ReforeSmart: Rethinking Forest landscape Sustainability through Multifractal Analysis Reforestation Techniques" under grant 2024-0052. The authors acknowledge support from the European Union NextGenerationEU and RD 289/2021 and the support of Project No. PGC2018-093854-B-I00 of the Ministerio de Ciencia, Innovación y Universidades de España. Support was also provided through KU Leuven internal grants STG/21/027 and OFC2023 and the University Institute for Research in Environmental Sciences of Aragon (IUCA) of the University of Zaragoza, as well as the Government of Aragon (Geoforest S51_23R).

Author contributions

Conceptualisation, A.U.C., and D.A.R.T.; methodology, A.U.C. and D.A.R.T.; formal analysis, A.U.C., A.M.T.A.; investigation, A.U.C., and A.G.; resources, A.U.C., J.d.l.R.; data curation, A.U.C. and D.A.R.T.; writing—original draft preparation, A.U.C.; writing—review and editing, A.G., J.d.l.R., and A.M.T.A.; visualisation, A.U.C.; supervision, J.d.l.R. All authors have read and approved the manuscript.

Declarations

Competing interests

The authors declare no competing interests.

Additional information

Correspondence and requests for materials should be addressed to J.R.F.